Original Article
EPIDEMIOLOGY/GENETICS

Obesity

Genetic Fine-Mapping and Identification of Candidate Genes and Variants for Adiposity Traits in Outbred Rats

Gregory R. Keele[1], Jeremy W. Prokop[2], Hong He[3], Katie Holl[3], John Littrell[3], Aaron Deal[4], Sanja Francic[5], Leilei Cui[5], Daniel M. Gatti[6], Karl W. Broman[7], Michael Tschannen[3], Shirng-Wern Tsaih[3], Maie Zagloul[1], Yunjung Kim[1], Brittany Baur[3], Joseph Fox[3], Melanie Robinson[2], Shawn Levy[2], Michael J. Flister[3], Richard Mott[5], William Valdar[1], and Leah C. Solberg Woods[4]**

Objective: Obesity is a major risk factor for multiple diseases and is in part heritable, yet the majority of causative genetic variants that drive excessive adiposity remain unknown. Here, outbred heterogeneous stock (HS) rats were used in controlled environmental conditions to fine-map novel genetic modifiers of adiposity.
Methods: Body weight and visceral fat pad weights were measured in male HS rats that were also genotyped genome-wide. Quantitative trait loci (QTL) were identified by genome-wide association of imputed single-nucleotide polymorphism (SNP) genotypes using a linear mixed effect model that accounts for unequal relatedness between the HS rats. Candidate genes were assessed by protein modeling and mediation analysis of expression for coding and noncoding variants, respectively.
Results: HS rats exhibited large variation in adiposity traits, which were highly heritable and correlated with metabolic health. Fine-mapping of fat pad weight and body weight revealed three QTL and prioritized five candidate genes. Fat pad weight was associated with missense SNPs in *Adcy3* and *Prlhr* and altered expression of *Krtcap3* and *Slc30a3*, whereas *Grid2* was identified as a candidate within the body weight locus.
Conclusions: These data demonstrate the power of HS rats for identification of known and novel heritable mediators of obesity traits.

Obesity (2018) **26**, 213-222. doi:10.1002/oby.22075

Introduction

Obesity and overweight are major risk factors for multiple cardiovascular and metabolic diseases (1). Of particular importance is visceral, or abdominal, adipose tissue, which is strongly predictive of metabolic health (2). Multiple environmental (e.g., lifestyle) and genetic factors contribute to obesity, with genetics accounting for up to 70% of the population variance for human BMI, obesity (3), and visceral adiposity (4). To date, human genome-wide association studies (GWAS) have identified many genes for anthropomorphic traits (5-8), but these genes explain only a small proportion of the heritable variation (5), indicating that many genes are yet unidentified. Identification of additional genes is particularly important because there has been a steady increase in prevalence of overweight and obesity since the 1970s (1), with more than one-third of adults and almost one-fifth of all children in the United States classified as having obesity (9).

One strategy for identifying the heritable modifiers of obesity is to control for exogenous environmental factors by using experimental genetic mapping strategies, such as the outbred heterogeneous stock (HS) rats. HS rats descend from eight inbred founder strains and have been outbred for more than 70 generations, such that the fine recombination block structure allows genetic mapping to identify regions that are only a few megabase pairs (10). In previous work, we used HS rats to fine-map a single region on rat chromosome 1 previously identified for glucose and insulin traits (11,12), and we identified *Tpcn2* as a likely causal gene at this locus (13). Here, we demonstrate that HS rats vary for adiposity traits, including body weight and visceral fat pad weight, and that these measures correlate with metabolic health. We then detect and fine-map quantitative trait loci (QTL) for these traits genome-wide and identify five likely causal genes within these loci.

[1] Department of Genetics, University of North Carolina at Chapel Hill, Chapel Hill, North Carolina, USA [2] HudsonAlpha Institute, Huntsville, Alabama, USA [3] Departments of Pediatrics and Physiology, Medical College of Wisconsin, Milwaukee, Wisconsin, USA [4] Department of Internal Medicine, School of Medicine, Wake Forest University, Winston Salem, North Carolina, USA. Correspondence: Leah C. Solberg Woods (lsolberg@wakehealth.edu)
[5] Genetics Institute, University College London, London, UK [6] Jackson Laboratory, Bar Harbor, Maine, USA [7] Department of Biostatistics and Medical Informatics, University of Wisconsin-Madison, Madison, Wisconsin, USA.

Funding agencies: This work was funded by R01 DK-088975, R01 DK-106386 (LCSW) and funding from the Individualized Medicine Institute at the Medical College of Wisconsin (LCSW). Partial support for GRK and YK was provided by R01 GM-104125 (WV). DMG and KWB were supported by R01 GM 070683. SWT and MJF were supported by R01 CA193343 (MJF). Protein modeling analysis was supported by the NIH Office of the Director award K01ES025435 (JWP).
Disclosure: The authors declared no conflict of interest.
*William Valdar and Leah C. Solberg Woods contributed equally to this study as senior authors.
Additional Supporting Information may be found in the online version of this article.
Received: 10 July 2017; **Accepted:** 21 October 2017; **Published online 28 November 2017. doi:10.1002/oby.22075**

Methods

Animals

HS colony. The NMcwi:HS colony, hereafter referred to as HS, was initiated by the NIH in 1984 by using the following eight inbred founder strains: ACI/N, BN/SsN, BUF/N, F344/N, M520/N, MR/N, WKY/N, and WN/N (14). This colony has been maintained at the Medical College of Wisconsin (MCW) since 2006 and has been through more than 70 generations of breeding. Rats were given *ad libitum* access to LabDiet 5010 diet (St. Louis, Missouri). Additional housing conditions are detailed in the Supporting Information Methods.

Founding inbred substrains. Other than M520/N (now maintained at MCW), phenotyping of the founders was conducted in the following substrains (abbreviated names to be used throughout manuscript in parentheses): ACI/Eur or ACI/Seg (ACI), BN/SsnHsd (BN), BUF/NHsd (BUF), F344/NHsd (F344), and WKY/NHsd (WKY). We tested 8 to 19 male rats per inbred strain.

Phenotyping protocol

We measured body weight at 16 weeks of age in 989 male HS rats. Rats underwent an intraperitoneal glucose tolerance test, as described previously (11,12). We used the Ascensia Elite system for reading blood glucose values (Bayer, Elkhart, Indiana). Plasma insulin levels were determined by using an ultrasensitive enzyme-linked immunosorbent assay (ELISA) kit (ALPCO Diagnostics, Salem, New Hampshire). The following metabolic measures were calculated: area under the curve (AUC) for glucose and insulin during the intraperitoneal glucose tolerance test, the quantitative insulin sensitivity check as a measure of insulin sensitivity, and the insulinogenic index as a measure of beta-cell sensitivity to glucose (12).

Inbreds and 743 HS rats were euthanized after an overnight fast at 17 weeks of age. Body weight and two measures of body length (from nose to base of the tail and from nose to end of tail) were collected, allowing us to calculate two measures of body mass index: BMI_Tail_Base and BMI_Tail_End. BMI was calculated as follows: $(\text{body weight} / \text{body length}^2) \times 10$. Rats were euthanized by decapitation and trunk blood was collected. Fasting cholesterol and triglycerides were determined from fasting serum on an ACE Alera autoanalyzer (Alfa Wassermann Diagnostic Technologies LLC, West Caldwell, New Jersey) by using an enzymatic method for detection. Several tissues were dissected and weighed, including retroperitoneal and epididymal visceral fat pads, hereafter referred to as RetroFat and EpiFat, respectively. Liver tissue was snap-frozen in liquid nitrogen for subsequent expression analysis. All protocols were approved by the Institutional Animal Care and Use Committee at MCW. Phenotyping data have been deposited in the Rat Genome Database (www.rgd.mcw.edu).

Genotyping

We extracted DNA from tail tissue from HS and the original eight inbred founder strains (tissue obtained from the NIH) by using either the DNeasy kit (Qiagen, Valencia, California) or a phenol-chloroform extraction. Founder and HS rats were genotyped by using the Affymetrix GeneChip Targeted Genotyping technology (Santa Clara, California) on a custom 10K single-nucleotide polymorphism (SNP) array panel, as previously described (15), with marker locations based on rat genome assembly 6.0. One hundred forty-seven samples were genotyped by the Vanderbilt Microarray Shared Resource center at Vanderbilt University in Tennessee (currently VANTAGE: http://www.vantage.vanderbilt.edu) and the remaining 842 by HudsonAlpha Institute for Biotechnology (http://hudsonalpha.org). From the 10,846 SNPs on the array, 8,218 were informative and produced reliable genotypes in the HS rats. From these final informative markers, the average SNP spacing was 284 kilobase (kb), with an average heterozygosity of 25.68%. Principal component analysis was used to confirm that there were no systematic genotyping differences between the two centers (Supporting Information Figure S1).

RNA-seq

RNA was extracted from the liver of 398 HS rats by using TRIzol (Fisher Scientific, Hampton, New Hampshire). Illumina kits were used to create library preparations and RNA-seq was run on the Illumina HiSeq 2500. RSEM and Bowtie were used to align reads and compute transcript level expression abundance (Supporting Information Methods).

Statistical analysis

Estimating heritability of adiposity traits. Narrow-sense heritability was estimated for each transformed phenotype by using a Bayesian linear mixed model (LMM) implemented in integrated nested Laplace approximation (INLA) (16,17). The LMM included fixed effects representing time food deprived, order of tissue harvest, dissector (notably, dissector significantly affected EpiFat and BMI_Tail_Base), and a random "polygenic" effect, which represented the effect of overall relatedness (18). Heritability (h^2) was defined as the proportion of variance attributed to polygenic effects versus residual noise (Supporting Information Methods).

Genome-wide association. QTL were identified by the genome-wide association of imputed allele dosages of genotyped SNPs. A hidden Markov model (R/qtl2 version 0.4-21; Karl Broman, University of Wisconsin, Madison, Madison, Wisconsin) was used to infer each HS rat's haplotype mosaic and thereby obtain robust estimates of each SNP's genotype. Association tests were then performed, SNP by SNP, on each trait by using a frequentist version of the LMM described for estimating heritability but with an added SNP effect term. Tests of the SNP effect yielded P values that are here reported as the negative log to the base 10 (logP). Genome-wide significance thresholds for logP scores were estimated by parametric bootstrap samples from the fitted null (11,19). Linkage disequilibrium (LD) intervals for the detected QTL were defined by including neighboring markers that met a set level of LD, measured with the squared correlation coefficient r^2; we used $r^2 = 0.5$ to define intervals based on the plots of the SNP associations overlaid with LD information (Supporting Information Methods).

Fine-mapping and haplotype effect estimation at detected QTL. SNP variants within the LD interval were prioritized by using the multi-SNP method LLARRMA-dawg (20), which calculates for each SNP a resample model inclusion probability (RMIP): SNPs with high RMIPs represent strong, independent signals, and the existence of multiple SNPs with a high RMIP is consistent with the presence of multiple independent signals. To characterize each QTL signal, we used the Diploffect model (21), which estimates the relative contributions of alternate founder haplotypes (Supporting Information Methods).

Candidate gene identification. Two parallel approaches were used: (1) bioinformatic analysis and protein modeling of known

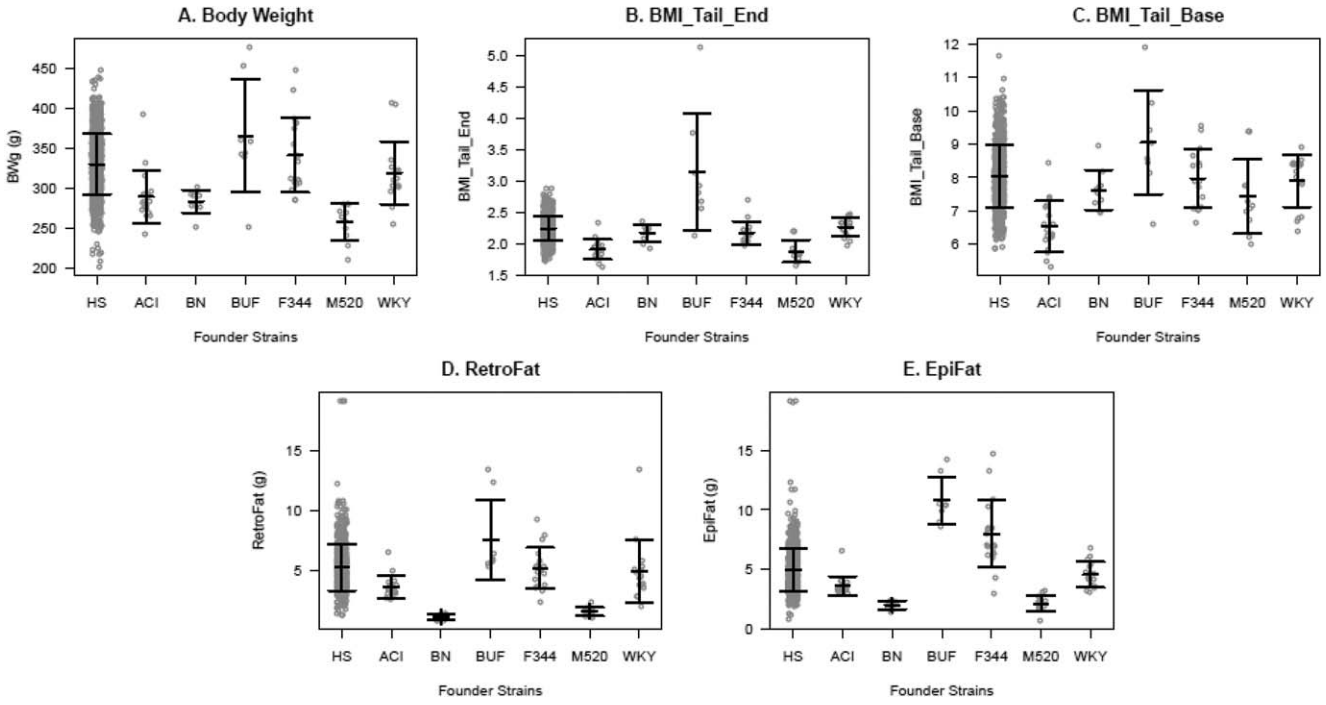

Figure 1 Adiposity traits in inbred founders and heterogeneous stock (HS) rats. Means ± SDs are shown. BMI was measured with length from the nose to the end of the tail (BMI_Tail_End) and from the nose to the base of the tail (BMI_Tail_Base). EpiFat and RetroFat are epididymal and retroperitoneal fat pad weight, respectively. Gray circles represent individual animals from 8 to 19 individuals from 6 of the founder strains and the HS rats (989 in body weight; 741 in RetroFat, EpiFat, and BMI_Tail_End; and 740 in BMI_Tail_Base). See text for statistical differences between founder strains.

sequence variants and (2) mediation analysis of expression levels. For (1), we used HS founder sequence (www.rgd.mcw.edu; genome build Rn6) to identify highly conserved, nonsynonymous coding variants within each QTL that were predicted to be damaging by PolyPhen (http://genetics.bwh.harvard.edu/pph/) and/or SIFT (www.sift.jcvi.org), focusing on variants in founder strains that showed haplotype effects at the locus. Variants were confirmed by using Sanger sequencing and then analyzed in the Sequence-to-Structure-to-Function analysis as previously described (22). Briefly, proteins were assessed with codon selection analysis of multiple species open reading frames, inspected for linear motif impact near variants of interest, and modeled with I-TASSER (23) and YASARA (24). Models were then assessed for likely impact on protein folding and/or function based on model confidence, phylogenetic sequence alignment, conservation, and whether or not the variant altered structural packing, molecular dynamic simulations, binding partners, linear motifs, or posttranslational modifications. For (2), transcript abundance levels of genes within HS liver were evaluated as potential causal mediators of the physiological QTL through mediation analysis (25) (Supporting Information Methods).

Results

HS founder strains exhibit large variation in adiposity traits

All phenotypes were rank-inverse normal transformed except for EpiFat, which instead was log transformed by using a method based on the Box-Cox procedure. All traits differed significantly between the inbred founder strains: body weight ($F_{5,76} = 15.492$, $P = 1.74e\text{-}10$), BMI_Tail_End ($F_{5,73} = 25.024$, $P = 1.34e\text{-}14$), BMI_Tail_Base ($F_{5,73} = 9.683$, $P = 4.02e\text{-}7$), EpiFat ($F_{5,78} = 69.541$, $P < 2.2e\text{-}16$), and RetroFat ($F_{5,78} = 38.157$, $P < 2.2e\text{-}16$; Figure 1). The BUF inbred strain had significantly more EpiFat mass (Tukey-Kramer $P \leq 0.05$) and BMI_Tail_End (Tukey-Kramer $P < 0.05$) relative to all other strains. BUF also had significantly more RetroFat mass compared with all strains (Tukey-Kramer $P < 0.001$) except F344 (Tukey-Kramer $P = 0.06175$); higher body weight relative to ACI, BN, and M520 (Tukey-Kramer $P < 0.01$); and higher BMI_Tail_Base than ACI and M520 (Tukey-Kramer $P < 0.05$). ACI, BN, and M520 were the lightest strains, with BN and M520 showing significantly lighter EpiFat (Tukey-Kramer $P \leq 1e\text{-}5$) and RetroFat (Tukey-Kramer $P \leq 0.001$) relative to other strains.

Adiposity traits are highly correlated with measures of metabolic health in HS rats

Variation between the founder strains is represented within the HS colony (Figure 1). Adiposity measures were highly correlated with several measures of metabolic health (Table 1, Figure 2). EpiFat significantly correlated with every measure of metabolic health, and RetroFat correlated with all but fasting glucose. Body weight significantly correlated with all measures except fasting triglycerides. BMI_Tail_End significantly correlated with fasting total cholesterol, fasting triglycerides, glucose AUC, insulin AUC, and insulinogenic index, whereas BMI_Tail_Base did not significantly correlate with any of the measures of metabolic health.

TABLE 1 Correlations between adiposity traits and measures of metabolic health in HS rats

	Body weight	BMI_Tail_End	BMI_Tail_Base	EpiFat	RetroFat
Fasting glucose	**0.1453 (0.0012)**	0.0952 (0.76)	0.0886 (1)	**0.1931 (3.24e-05)**	0.1132 (0.1009)
Fasting insulin	**0.1936 (3.48-07)**	0.1153 (0.091)	−0.0248 (1)	**0.4314 (1.35e-31)**	**0.3516 (4.75e-27)**
Fasting total cholesterol	**0.2644 (7.10e-11)**	**0.2428 (5.75e-09)**	0.1172 (0.39)	**0.2535 (6.85e-10)**	**0.3529 (1.02e-20)**
Fasting triglycerides	0.1291 (0.12)	**0.2426 (6.07e-09)**	0.0950 (1)	**0.3096 (1.75e-15)**	**0.3499 (2.55e-20)**
Glucose AUC	**0.1378 (0.0040)**	**0.1259 (0.0214)**	0.0652 (1)	**0.1663 (0.0016)**	**0.1718 (1.71e-05)**
Insulin AUC	**0.2937 (5.67e-18)**	**0.2238 (7.99e-10)**	0.0312 (1)	**0.4670 (2.71e-37)**	**0.4397 (8.79e-44)**
QUICKI	**−0.2042 (3.91e-08)**	−0.1198 (0.0523)	0.0211 (1)	**−0.4338 (5.24e-32)**	**−0.3544 (1.57e-27)**
IGI	**0.1629 (0.0001)**	**0.1220 (0.0430)**	0.0001 (1)	**0.2475 (5.46e-09)**	**0.2038 (5.46e-08)**

Spearman's rank correlation with Bonferonni-adjusted *P* values in parentheses (bold if < 0.05). To mitigate potentially confounding effects of experimental covariates, correlations performed on phenotypic residuals (i.e., on the residuals after regressing out covariate effects from the rank-inverse normal transformed phenotype).
AUC, area under the curve; BMI_Tail_Base, BMI with length from the nose to the base of the tail; BMI_Tail_End, BMI with length from the nose to the end of the tail; EpiFat, epididymal fat pad weight; HS, heterogeneous stock; IGI, insulinogenic index; QUICKI, quantitative insulin sensitivity check; RetroFat, retroperitoneal fat pad weight.

Adiposity traits are highly heritable

Adiposity traits were highly heritable in HS rats: body weight (posterior mode of $h^2 = 75.3\%$; 95% highest posterior density interval = 67.0%-81.7%), EpiFat (54.1%; 40.1%-66.0%), RetroFat (53.9%; 39.7%-66.7%), BMI_Tail_End (45.0%; 32.3%-57.2%) and BMI_Tail_Base (25.4%; 13.6%-41.8%).

RetroFat QTL on chromosomes 1 and 6

Two 90% significant QTL were identified for RetroFat, a QTL on rat chromosome 6: 22.79-28.93 megabase (Mb) (6.14 Mb, −logP = 4.73) and a QTL on chromosome 1: 280.63-281.82 Mb (1.19 Mb, −logP = 4.69; Figure 3A-3C, Figure 6A-6C). The LLARRMA-dawg multi-SNP fine-mapping analysis narrowed the most likely region of the broader chromosome 6 QTL to a 1.46 Mb region (27.17-28.63 Mb; Supporting Information Figure S2), narrowing the number of the genes from 130 to 30 (Supporting Information Table S1, Supporting Information Figure S3). Estimating founder haplotype effects at the chromosome 6 QTL gave an effect size (posterior median) of 11.05% and showed that, at this locus, decreased fat pad weight was associated with the WKY haplotype (Figure 3D). For the chromosome 1 QTL, the effect size was 13.33%, with increased fat pad weight associated with BUF, MR, and WKY haplotypes (Figure 6D).

Identification of *Adcy3, Krtcap3*, and *Slc30a3* within the chromosome 6 RetroFat QTL

Within the chromosome 6 RetroFat QTL, bioinformatic analysis revealed only one gene, *Adcy3*, that had a highly conserved, potentially damaging, nonsynonymous variant in the WKY rat, the founder haplotype associated with decreased RetroFat at this locus. *Adcy3* also falls within the fine-mapped support interval of the QTL (Figure 3C). The WKY founder strain harbors a C at position 28,572,363 base pairs (bp) within *Adcy3*, whereas all other strains harbor a T, resulting in a leucine-to-proline substitution at amino acid 121. On the basis of DNA information from 86 nucleotide

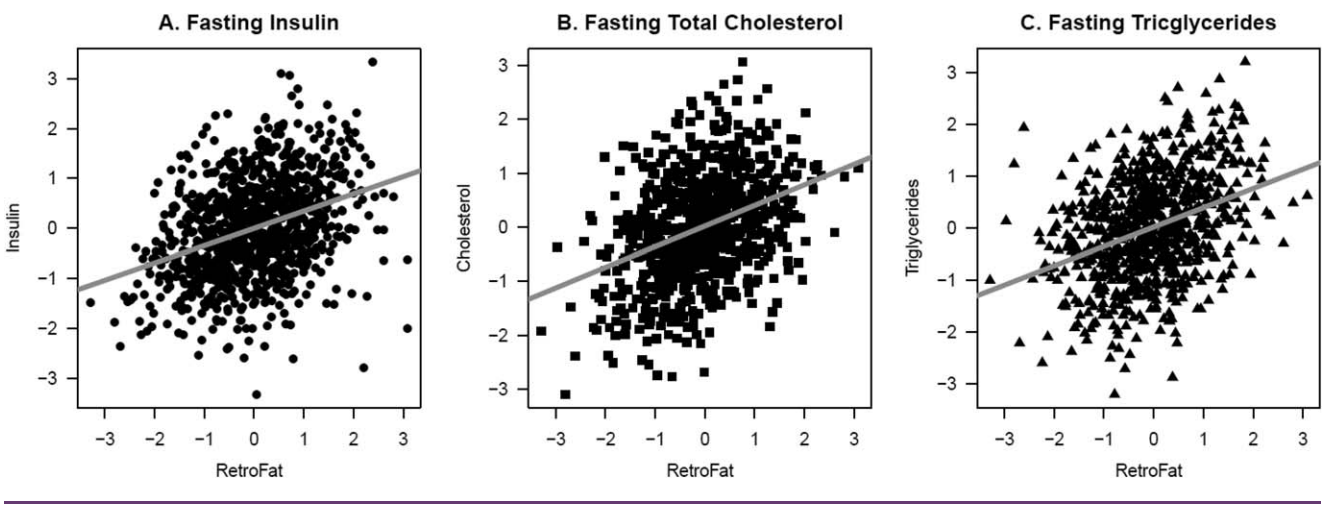

Figure 2 Significant correlations between retroperitoneal fat pad weight (RetroFat) and (**A**) fasting insulin ($P = 4.75e\text{-}27$), (**B**) fasting total cholesterol ($P = 1.02e\text{-}20$), and (**C**) fasting triglycerides ($P = 2.55e\text{-}20$) in heterogeneous stock (HS) rats. Plots show the residuals of rank-inverse normal transformed phenotypes with nuisance factors regressed out to restrict correlation estimates to that between RetroFat and these metabolic traits. Significant correlations were also found between RetroFat and several other measures of metabolic health (see Table 1).

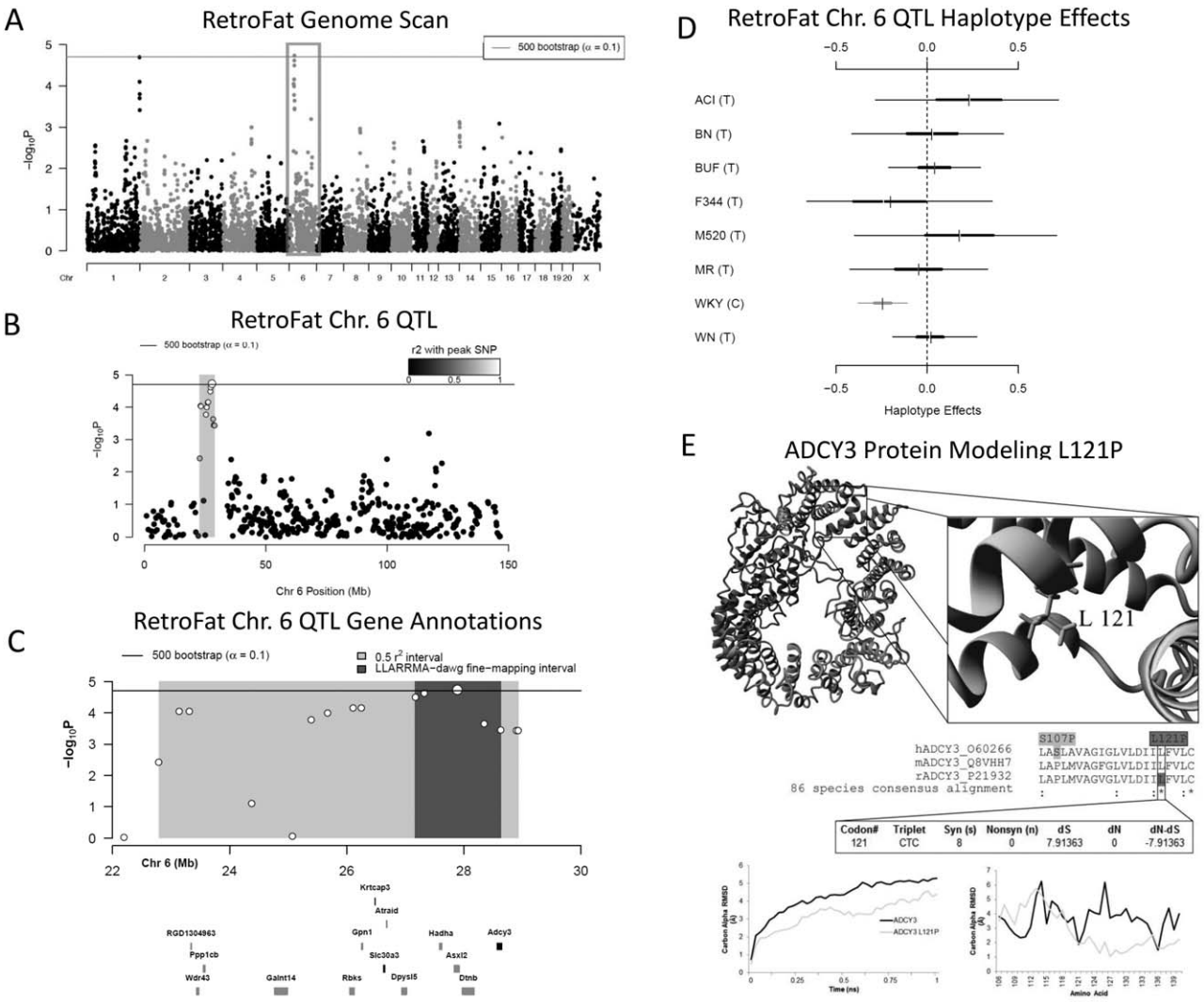

Figure 3 (**A**) Genome scan of retroperitoneal fat pad weight (RetroFat). The *x*-axis is the position on the chromosome, and the *y*-axis is the −logP level of association. Genome-wide significance thresholds were calculated by using parametric bootstraps from the null model ($\alpha = 0.1$; logP = 4.70). (**B**) The gray region highlights the 6.14 linkage disequilibrium support interval of the chromosome 6 quantitative trait loci (QTL), showing neighboring markers that were correlated with the peak marker, which represent genomic regions likely to contain the causal variant underlying the statistical signal. (**C**) Annotation of genes that fall within the support interval. The entire 6.14 region is shaded in gray, with the fine-mapped 1.46 Mb region shaded in dark gray. Only genes that have a cis-expression QTL are shown. All 130 genes within the region are listed in Supporting Information Table S1. (**D**) Additive haplotype effects were estimated by using the Diploffect model, which takes into account uncertainty in haplotype state. Single-nucleotide polymorphism (SNP) allele information is overlaid on the haplotype effects and are distinguished by black or gray. The WKY haplotype, the only haplotype with the C allele at the chromosome 6 locus, had a significantly negative effect on phenotype. (**E**) Protein modeling for ADCY3. Variant L121P of ADCY3 is found with the conserved hydrophobic core of the transmembrane helices. A zoomed in view is shown to the right. The middle panel shows sequence alignments of amino acids. ADCY3 amino acid 121 is also 100% conserved as a leucine in 86 analyzed vertebrate species. A human SNP is known at amino acid 107. Using the DNA information from the 86 nucleotide sequences for ADCY3, there was also evidence of selective pressure in the DNA sequence to conserve the amino acid. The bottom panel shows molecular dynamic simulations for ADCY3. Simulations performed on the protein dimer for wild type (WT, black) or the mutant (ADCY3 L121P, gray) suggested that the models' average movement over time was altered. Altered movement was seen in the simulations for ADCY3, with fluctuation of amino acids found near amino acid 121 when mutated.

sequences for ADCY3, it appears that this variant is highly conserved with evidence for selective pressure. Protein modeling indicated that amino acid 121 is located within the first transmembrane region, with a proline likely causing a bend in the helix and thus altered transmembrane packing (Figure 3E).

Because fine-mapping supported multiple independent signals at the QTL, we investigated potential mediators among the cis-expressed genes. Mediation analysis identified six potential mediators, all driven by the WKY haplotype (Figure 4; Supporting Information Tables S4-S5), suggesting that multiple genes may influence RetroFat at this locus. Two in particular were strongly supported: *Krtcap3* as a full mediator and *Slc30a3* as a partial mediator, remaining significant after controlling for *Krtcap3*. Under the proposed model (Figure 5), the WKY haplotype increases expression of *Krtcap3*, which was itself negatively correlated with RetroFat (Supporting

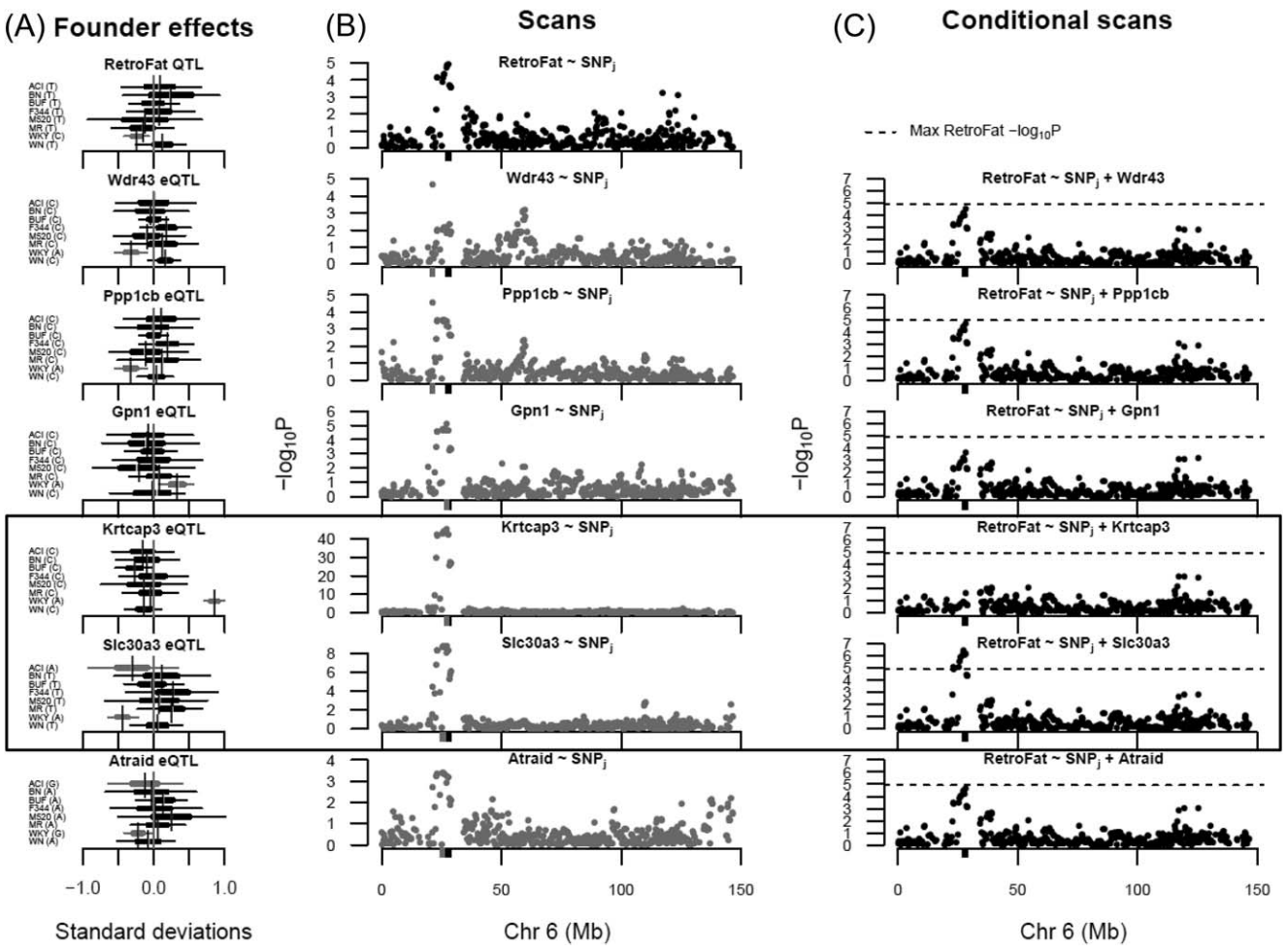

Figure 4 Mediation analysis identified the expression levels of six genes (*Wdr43, Ppp1cb, Gpn1, Krtcap3, Slc30a3*, and *Atraid*; Supporting Information Table S5) in the retroperitoneal fat pat weight (RetroFat) chromosome 6 quantitative trait loci (QTL) interval as potential mediators of the QTL effect on the phenotype. (**A**) The haplotype effects on RetroFat at the QTL and on the mediators at the expression QTL revealed that in this region, the WKY haplotype was largely driving the differences in RetroFat and mediator gene expression, suggesting a possible connection between RetroFat and local gene expression. (**B**) Comparisons of the RetroFat chromosome 6 association scan with association scans for the potential mediators revealed them to likely have colocalizing cis-expression QTL with the RetroFat QTL. (**C**) RetroFat chromosome 6 association scans, conditioned on candidate gene expression, were consistent with the mediation analysis finding that *Krtcap3* was a strong candidate as full mediator of the effect of QTL on RetroFat. When *Krtcap3* expression was included in the model, the QTL was largely removed. *Slc30a3*, as a potential suppressor of the QTL effect on RetroFat, actually increased the significance seen at the QTL.

Information Figure S4); thus, the causal path is consistent with the negative WKY effect on RetroFat at the locus. Meanwhile, WKY decreases expression of *Slc30a3*, which was also negatively correlated with RetroFat, suggesting that *Slc30a3* is a suppressor of the QTL/*Krtcap3* effect.

Identification of *Prlhr* within the chromosome 1 RetroFat QTL

Within the chromosome 1 RetroFat QTL, there are 15 genes, 10 of which are uncharacterized (Figure 6B-6C, Supporting Information Table S2). One gene, *Prlhr*, contains a nonsynonymous variant in the BUF and WKY founder strains, two founder haplotypes associated with increased fat pad weight at this locus. The variant falls within the start codon, changing methionine to isoleucine. The next methionine falls at amino acid 65, such that the conserved N-terminal region and half of transmembrane helix 1 would be deleted with the variant (Figure 4E, https://youtu.be/vRTIkITXRbw). A molecular dynamic simulation of the PRLHR protein with and without the first 64 amino acids showed strong changes to the entire GPCR transmembrane region. *Prlhr* is expressed mainly in adrenal and brain tissue, such that expression levels could not be determined in liver tissue. None of the liver-expressed genes local to the QTL map as cis-expression QTL; thus, *Prlhr* remains the strongest candidate within this region.

Body weight QTL on chromosome 4 and identification of *Grid2*

A 95% significant QTL for body weight was also detected on rat chromosome 4: 91.35 Mb to 94.7 Mb (3.35 Mb, $-\log P = 5.32$) (Figure 7A-7C). At this locus, whose effect size was 12.33%, decreases in body weight were associated with ACI, BUF, F344, and MR haplotypes, and increases were associated with BN (Figure 7D).

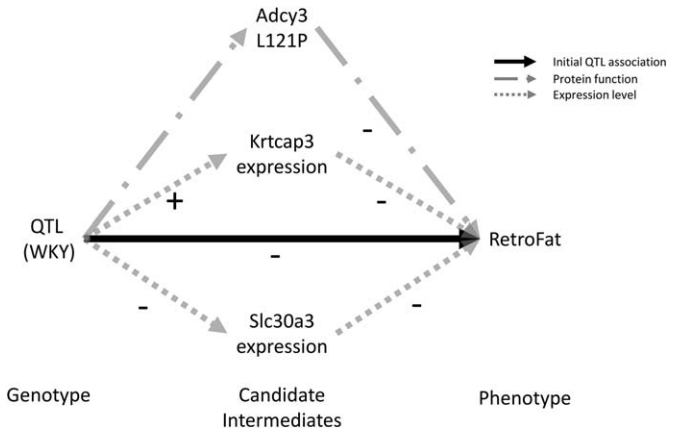

Figure 5 Model demonstrating the role of *Adcy3, Krtcap3*, and *Slc30a3* on retroperitoneal fat pad weight (RetroFat). WKY haplotype increases the expression of *Krtcap3*, which was itself negatively correlated with RetroFat (Supporting Information Figure S4); thus, the causal path was consistent with the negative WKY effect on RetroFat at the locus. In contrast, WKY decreases expression of *Slc30a3*, which was also negatively correlated with RetroFat, suggesting that *Slc30a3* was suppressor of the quantitative trait loci (QTL)/*Krtcap3* effect. Finally, the nonsynonymous variant with *Adcy3* causesd amino acid change to L121P, leading to lower RetroFat.

Within the body weight QTL, there are only 11 genes, 9 of which are pseudogenes or uncharacterized LOC proteins, leaving only *Ccser1* and *Grid2* (Figure 7C, Supporting Information Table S3). None of the genes at this locus contained highly conserved potentially damaging nonsynonymous variants. Both *Ccser1* and *LOC108350839* are expressed in liver, but neither's expression was significantly associated with the body weight QTL, ruling these out as candidate mediators. The brain-specific *Grid2* is the only gene that has previously been linked to body weight (26), and *Grid1* was recently associated with BMI in human GWAS (5), implicating *Grid2* as the most likely candidate at this locus.

Discussion

This study is the first to use HS rats for mapping adiposity traits genome-wide, demonstrating their utility for uncovering genes and variants likely to impact human adiposity. We identified QTL for RetroFat on rat chromosomes 1 and 6 and a QTL for body weight on chromosome 4. By using various fine-mapping procedures, we identified three likely candidate genes within the chromosome 6 RetroFat locus: a protein-coding variant within *Adcy3* and transcriptional regulation of *Krtcap3* and *Slc30a3*. Within the chromosome 1 RetroFat QTL, we identified a variant within *Prlhr* that increases fat pad weight. Lastly, *Grid2* was identified as the most likely candidate gene within the body weight locus. It is of interest that several of these candidate genes play a role in neural regulation of energy metabolism and/or feeding behavior.

As expected, both the HS founders and the HS population varied for adiposity traits, with BUF showing the highest adiposity and ACI, BN, and M520 showing the lowest. As seen in humans (3,4), these traits were highly heritable. Also similar to that in humans (2), increased body weight in HS rats, particularly visceral fat pad weight (RetroFat and EpiFat), was significantly associated with several measures of metabolic health, indicating that genes underlying QTL for adiposity traits are likely to contribute to overall metabolic health in HS rats.

Despite high heritability for adiposity traits in this model, we found only three QTL for the five traits that were studied. The remaining heritability could be attributable to loci of small effect and/or complex genetic architecture that lie below the limit of detection in this study, and this accords with the fact that the QTL we identified were each of relatively large effect (12.33%, 13.33%, and 11.05%, respectively). The identified QTL also had relatively small LD support intervals (3.35 Mb, 1.19 Mb, and 6.14 Mb, respectively), significantly decreasing the number of potential candidate genes within each QTL relative to traditional QTL studies using F2 intercross or backcross animals; the map density, however, was too low for high resolution mapping of the genes within the interval. We expect that increasing both the number of animals used as well as the density of genotyping would serve to uncover additional loci.

The chromosome 6 RetroFat locus encompassed 6.14 Mb, contained 130 genes, and was driven by the WKY haplotype. Using a fine-mapping procedure that allowed for the presence of multiple signals, we identified a 1.46 Mb plausible region for the QTL. *Adcy3* was the only gene in this region to contain a highly conserved, nonsynonymous variant in the WKY founder strain that is predicted to be damaging: the leucine-to-proline switch at amino acid 121 would likely induce a bend in the helix, leading to altered membrane interactions and binding. In addition, we found that multiple genes within the locus map as expression QTL. Subsequent mediation analysis supported roles for *Krtcap3* and *Slc30a3*, with *Krtcap3* expression presenting as a full mediator of the QTL and *Slc30a3* expression as a partial/suppressor mediator. Although little is known about *Krtcap3, Slc30a3* is a zinc transporter that plays a role in glucose transport and metabolism (27), and *Adcy3* is an enzyme that catalyzes the cyclic adenosine monophosphate second messenger system and is likely involved in energy homeostasis (28). The *POMC*/*RBJ*/*ADCY3* region has previously been identified in multiple human GWAS for BMI and obesity (8,29-31). Interestingly, a nonsynonymous amino acid change (Ser107Pro) in the human *Adcy3* gene (8), which falls within the same transmembrane helix as the rat variant, has been identified as the causal variant in height-adjusted childhood BMI (30), indicating the same likely causal variant between rats and humans. *Adcy3* knock-out and haplo-insufficient mice develop obesity with age, exhibiting increased food intake and decreased locomotion (32,33). In addition, gain of function in *Adcy3* protects against diet-induced obesity (34), further supporting a causal role for this gene.

The chromosome 1 RetroFat locus encompassed 1.19 Mb and contained 15 genes, with BUF, MR, and WKY haplotypes increasing RetroFat. *Prlhr*, containing a nonsynonymous variant in both the BUF and WKY strains, stood out as the most likely candidate gene: the variant falls within the methionine start site and leads to removal of the conserved N-terminal region and half of transmembrane helix 1, likely having a large impact on protein function. This variant is found in several other rat strains including FHH, GK, LEW, and SD. *Prlhr* is known to play a role in feeding behavior, with intracerebroventricular administration in the hypothalamus leading to decreased food intake (35) and *Prlhr* knock-out mice exhibiting

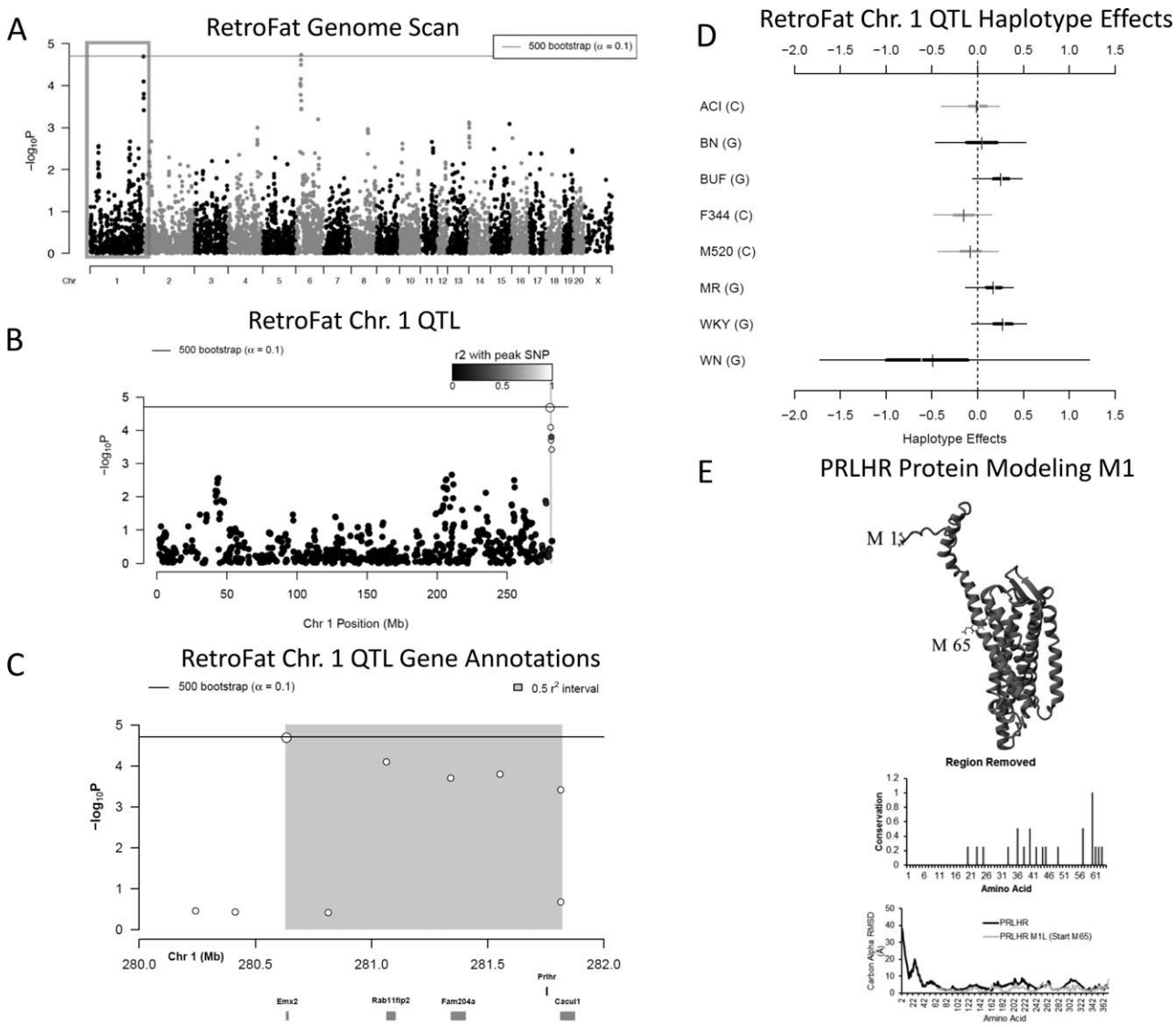

Figure 6 (**A**) Genome scan of retroperitoneal fat pad weight (RetroFat) as described in Figure 3A. (**B**) The gray region highlights the 1.19 Mb linkage disequilibrium support interval for the chromosome 1 locus representing neighboring markers that were correlated with the peak marker, which represent genomic regions likely to contain the causal variant underlying the statistical signal. (**C**) Annotation of the five characterized genes that fall within the support interval. (**D**) Additive founder haplotype effects for the chromosome 1 RetroFat locus. Additive haplotype effects were estimated by using the Diploffect model, which takes into account uncertainty in haplotype state. Single-nucleotide polymorphism (SNP) allele information was also overlaid on the haplotype effects. The C allele was shared by ACI, F344, and M520, which possesses a variant with a negative effect on RetroFat, whereas BUF, MR, and WKY haplotypes resulted in increased RetroFat at this locus. (**E**) Protein modeling for PRLHR. Variant M1I of PRLHR is found within the methionine start site. The next start site is at position 65, leading to removal of the conserved N-terminal region and half of transmembrane helix 1. Sixteen amino acids removed were under selective pressure (middle panel), and the deletion of the first 64 amino acids caused a destabilization of the entire protein dynamics as seen by the molecular dynamic simulations (bottom panel).

increased food intake, body weight, and fat pad weight (36). Interestingly, this specific variant did not alter feeding behavior in outbred Sprague-Dawley rats (37), indicating that the effect of the variant on fat pad weight may be independent of food intake, although additional studies are needed to confirm this.

The body weight locus encompassed 3.35 Mb and contained 11 genes, none of which contained highly conserved nonsynonymous variants predicted to be damaging between the two haplotype effect groups: ACI, BUR, F344, and MR versus BN. Only one gene in the region, *Grid2*, has previously been linked to obesity, jointly with tobacco use, in a family-based study (26), making it the most likely candidate gene. Interestingly, *Grid1* was associated with BMI in a recent human GWAS (5), further supporting a potentially causal role for *Grid2* within the rat body weight locus. *Grid2* encodes the glutamate ionotropic receptor delta type subunit 2 and is known to play a role in synapse formation, particularly within the cerebellum (38). Synaptic formation and plasticity are increasingly being recognized

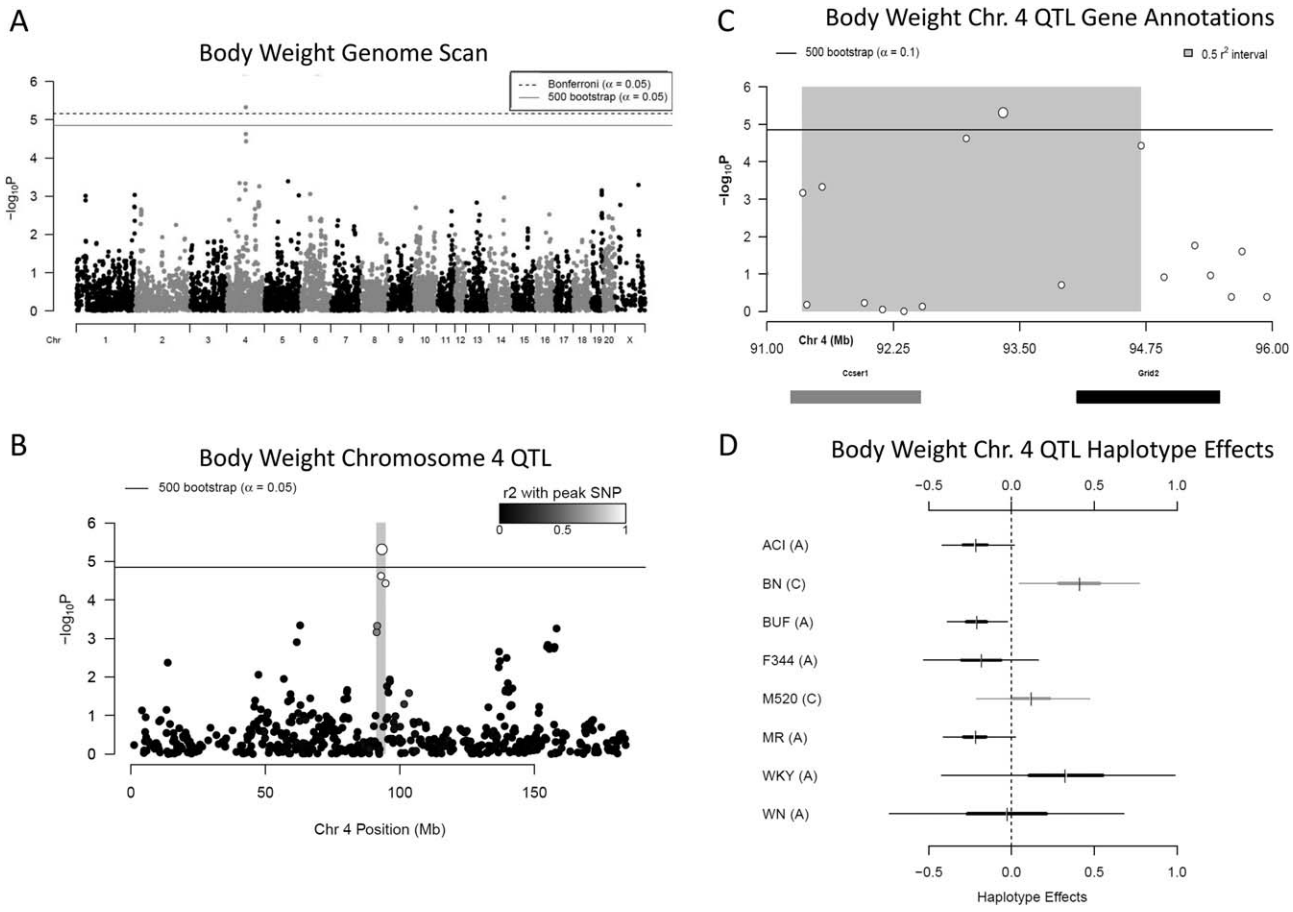

Figure 7 (**A**) Genome scan of body weight. The *x*-axis is the position on the chromosome and the *y*-axis is the −logP level of association. Genome-wide significance thresholds were calculated by using parametric bootstraps from the null model (significant: $\alpha = 0.05$, logP = 4.86) and conservative $\alpha = 0.05$ Bonferroni thresholds (logP = 5.16). (**B**) The linkage disequilibrium support interval in gray is 3.35 Mb. (**C**) Annotation of the two characterized genes that fall within the support interval. (**D**) Additive haplotype effects for chromosome 4 body weight quantitative trait loci (QTL). The C allele at the marker could represent shared haplotype descent between BN and M520, both of which had an increasing effect on body weight at this locus. ACI, BUF, F344, and MR haplotypes had a decreasing effect on body weight at this locus, all of which share the A allele. The WKY and WN also have an A allele, and the WKY haplotype had an increasing effect on body weight, whereas the WN haplotype appears not to affect body weight, although the credible interval of both is fairly large and not well represented in the data at this locus.

as playing a role in metabolism and energy balance (39). Additional work, including assessing *Grid2* expression levels in brain tissue, is needed to confirm or eliminate *Grid2* as the causal gene at this locus.

In summary, we have used HS rats to identify QTL for adiposity traits, leading to identification of five candidate genes and two likely causal variants. Some genes have previously been identified in human GWAS or linkage studies (*Adcy3, Grid2*) or implicated in rodent models of obesity (*Adcy3, Prlhr*), whereas two genes are novel (*Krtcap3, Slc30a3*). The *Adcy3* variant falls within the same transmembrane helix as that found in humans, indicating the direct human relevance of this work. It is also of interest that *Adcy3, Prlhr*, and *Grid2* have previously been found to impact feeding behavior and/or neural regulation of metabolism. This work demonstrates the power of HS rats for genetic fine-mapping and identification of underlying candidate genes and variants that will likely be relevant to human adiposity.

Acknowledgments

We would like to thank Jennifer Phillips for running the cholesterol and triglyceride assays. We would like to thank Mary Shimoyama and Jeffrey DePons for help in transferring founder sequence to Rn6 in the Rat Genome Database.

References

1. Wang YC, McPherson K, Marsh T, Gortmaker SL, Brown M. Health and economic burden of the projected obesity trends in the USA and the UK. *Lancet* 2011;378:815-825.
2. Emdin CA, Khera AV, Natarajan P, et al. Genetic association of waist-to-hip ratio with cardiometabolic traits, type 2 diabetes, and coronary heart disease. *JAMA* 2017;317:626-634.
3. Stunkard AJ, Foch TT, Hrubec Z. A twin study of human obesity. *JAMA* 1986;256:51-54.
4. Katzmarzyk PT, Malina RM, Pérusse L, et al. Familial resemblance in fatness and fat distribution. *Am J Hum Biol* 2000;12:395-404.

5. Locke AE, Kahali B, Berndt SI, et al. Genetic studies of body mass index yield new insights for obesity biology. *Nature* 2015;518:197-206.
6. Lu Y, Day FR, Gustafsson S, et al. New loci for body fat percentage reveal link between adiposity and cardiometabolic disease risk. *Nat Commun* 2016;7:10495. doi: 10.1038/ncomms10495
7. Ng MCY, Graff M, Lu Y, et al. Discovery and fine-mapping of adiposity loci using high density imputation of genome-wide association studies in individuals of African ancestry: African Ancestry Anthropometry Genetics Consortium. *PLoS Genet* 2017;13: e1006719. doi: 10.1371/journal.pgen.1006719
8. Speliotes EK, Willer CJ, Berndt SI, et al. Association analyses of 249,796 individuals reveal 18 new loci associated with body mass index. *Nat Genet* 2010; 42:937-948.
9. Flegal KM1, Kruszon-Moran D, Carroll MD, Fryar CD, Ogden CL. Trends in obesity among adults in the United States, 2005 to 2014. *JAMA* 2016;315:2284-2291.
10. Solberg Woods LC. QTL mapping in outbred populations: successes and challenges. *Physiol Genomics* 2014;46:81-90.
11. Solberg Woods LC, Holl K, Tschannen M, Valdar W. Fine-mapping a locus for glucose tolerance using heterogeneous stock rats. *Physiol Genomics* 2010;41: 102-108.
12. Solberg Woods LC, Holl KL, Oreper D, Xie Y, Tsaih SW, Valdar W. Fine-mapping diabetes-related traits, including insulin resistance, in heterogeneous stock rats. *Physiol Genomics* 2012;44:1013-1026.
13. Tsaih SW, Holl K, Jia S, et al. Identification of a novel gene for diabetic traits in rats, mice, and humans. *Genetics* 2014;198:17-29.
14. Hansen C, Spuhler K. Development of the National Institutes of Health genetically heterogeneous rat stock. *Alcohol Clin Exp Res* 1984;8:477-479.
15. STAR Consortium; Saar K, Beck A, Bihoreau MT, et al. SNP and haplotype mapping for genetic analysis in the rat. *Nat Genet* 2008;40:560-566.
16. Holand AM, Steinsland I, Martino S, Jensen H. Animal models and integrated nested Laplace approximations. *G3 (Bethesda)* 2013;3:1241-1251.
17. Rue H, Martino S, Chopin N. Approximate Bayesian inference for latent Gaussian models by using integrated nested Laplace approximations. *J R Stat Soc Series B Stat Methodol* 2009;71:319-392.
18. Gatti DM, Svenson KL, Shabalin A, et al. Quantitative trait locus mapping methods for diversity outbred mice. *G3 (Bethesda)* 2014;4:1623-1633.
19. Valdar W, Holmes CC, Mott R, Flint J. Mapping in structured populations by resample model averaging. *Genetics* 2009;182:1263-1277.
20. Sabourin J, Nobel AB, Valdar W. Fine-mapping additive and dominant SNP effects using group-LASSO and fractional resample model averaging. *Genet Epidemiol* 2015;39:77-88.
21. Zhang Z, Wang W, Valdar W. Bayesian modeling of haplotype effects in multiparent populations. *Genetics* 2014;198:139-156.
22. Prokop JW, Lazar J, Crapitto G, Smith DC, Worthey EA, Jacob HJ. Molecular modeling in the age of clinical genomics, the enterprise of the next generation. *J Mol Model* 2017;23:75. doi: 10.1007/s00894-017-3258-3
23. Roy A, Kucukural A, Zhang Y. I-TASSER: a unified platform for automated protein structure and function prediction. *Nat Protoc* 2010;5:725-738.
24. Krieger E, Joo K, Lee J, et al. Improving physical realism, stereochemistry, and side-chain accuracy in homology modeling: four approaches that performed well in CASP8. *Proteins* 2009;77 Suppl 9:114-122.
25. Baron RM, Kenny DA. The moderator-mediator variable distinction in social psychological research: conceptual, strategic, and statistical considerations. *J Pers Soc Psychol* 1986;51:1173-1182.
26. Nikpay M, Šeda O, Tremblay J, et al. Genetic mapping of habitual substance use, obesity-related traits, responses to mental and physical stress, and heart rate and blood pressure measurements reveals shared genes that are overrepresented in the neural synapse. *Hypertens Res* 2012;35:585-591.
27. Smidt K, Jessen N, Petersen AB, et al. SLC30A3 responds to glucose- and zinc variations in beta-cells and is critical for insulin production and *in vivo* glucose-metabolism during beta-cell stress. *PLoS One* 2009;4:e5684. doi: 10.1371/journal.pone.0005684
28. Wu L, Shen C, Seed Ahmed M, Östenson CG, Gu HF. Adenylate cyclase 3: a new target for anti-obesity drug development. *Obes Rev* 2016;17:907-914.
29. Nordman S, Abulaiti A, Hilding A, et al. Genetic variation of the adenylyl cyclase 3 (AC3) locus and its influence on type 2 diabetes and obesity susceptibility in Swedish men. *Int J Obes (Lond)* 2008;32:407-412.
30. Stergiakouli E, Gaillard R, Tavaré JM, et al. Genome-wide association study of height-adjusted BMI in childhood identifies functional variant in ADCY3. *Obesity (Silver Spring)* 2014;22:2252-2259.
31. Wen W, Cho YS, Zheng W, et al. Meta-analysis identifies common variants associated with body mass index in east Asians. *Nat Genet* 2012;44:307-311.
32. Tong T, Shen Y, Lee HW, Yu R, Park T. Adenylyl cyclase 3 haploinsufficiency confers susceptibility to diet-induced obesity and insulin resistance in mice. *Sci Rep* 2016;6:34179. doi: 10.1038/srep34179
33. Wang Z, Li V, Chan GC, et al. Adult type 3 adenylyl cyclase-deficient mice are obese. *PLoS One* 2009;4:e6979. doi: 10.1371/journal.pone.0006979
34. Pitman JL, Wheeler MC, Lloyd DJ, Walker JR, Glynne RJ, Gekakis N. A gain-of-function mutation in adenylate cyclase 3 protects mice from diet-induced obesity. *PLoS One* 2014;9:e110226. doi: 10.1371/journal.pone.0110226
35. Lawrence CB, Celsi F, Brennand J, Luckman SM. Alternative role for prolactin-releasing peptide in the regulation of food intake. *Nat Neurosci* 2000;3:645-646.
36. Gu W, Geddes BJ, Zhang C, Foley KP, Stricker-Krongrad A. The prolactin-releasing peptide receptor (GPR10) regulates body weight homeostasis in mice. *J Mol Neurosci* 2004;22:93-103.
37. Ellacott KL, Donald EL, Clarkson P, et al. Characterization of a naturally-occurring polymorphism in the UHR-1 gene encoding the putative rat prolactin-releasing peptide receptor. *Peptides* 2005;26:675-681.
38. Hirai H, Launey T, Mikawa S. New role of delta2-glutamate receptors in AMPA receptor trafficking and cerebellar function. *Nat Neurosci* 2003;6:869-876.
39. Dietrich MO, Horvath TL. Hypothalamic control of energy balance: insights into the role of synaptic plasticity. *Trends Neurosci* 2013;36:65-73.